

1           **Comparison of the multifractal characteristics of heavy**  
2           **metals in soils within two areas of contrasting economic**  
3           **activities in China**

4 Xiaohui Li<sup>a, c</sup>, Feng Yuan<sup>b, a \*</sup>, Simon M. Jowitt<sup>d</sup>, Xianglin Li<sup>a</sup>, Taofa Zhou<sup>a, c</sup>, Jie  
5 Zhou<sup>a, c</sup>, Xunyu Hu<sup>a, c</sup>, Yang Li<sup>a, c</sup>

6 a. School of Resources and Environmental Engineering, Hefei University of  
7 Technology, Hefei 230009, China

8 b. Xinjiang Research Centre for Mineral Resources, Xinjiang Institute of Ecology and  
9 Geography, Chinese Academy of Sciences, Urumqi, Xinjiang 830011, China

10 c. Ore Deposit and Exploration Centre, Hefei University of Technology, Hefei  
11 230009, China

12 d. School of Earth, Atmosphere and Environment, Monash University, Wellington  
13 Road, Clayton, VIC 3800, Australia

14 \*Corresponding author: Email: [yf\\_hfut@163.com](mailto:yf_hfut@163.com), Tel: [+8605512901648](tel:+8605512901648)

15 **Abstract**

16       Industrial and agricultural activities can generate heavy metal pollution that  
17 causes a number of negative environmental and health impacts. This means that  
18 evaluating heavy metal pollution and identifying the sources of these pollutants,  
19 especially in urban or developed areas, is an important first step in mitigating the  
20 effects of these contaminating but necessary economic activities. Here, we present the  
21 results of a heavy metal (Cu, Pb, Zn, Cd, As and Hg) soil geochemical survey and use  
22 these data to evaluate and compare the characteristics of heavy metal pollution in soils  
23 within urban or developed areas. This survey focuses on Hefei, the provincial capital  
24 of Anhui Province, China, an area that contains a number of individual towns within a  
25 large municipal area. This study uses a multifractal spectral technique to identify the

26 multifractality in the geochemistry of soils within the industrial Daxing and  
27 agricultural Yicheng areas of Anhui Province. Determining three multifractal  
28 parameters ( $\Delta\alpha$ ,  $\Delta f(\alpha)$  and  $\tau''(1)$ ) for these soil geochemical data indicates that overall  
29 amount of multifractality within the soil geochemical data for the Daxing area  
30 decreases as follows: Pb>Cd>As>Zn>Hg>Cu, whereas the overall amount of  
31 multifractality within the soil geochemical data for the Yicheng area decreases as  
32 follows: Hg>Zn>As>Cd>Pb>Cu. These differences in the degree of multifractality  
33 indicates that the soils in these areas have differing multifractal geochemical  
34 characteristics, suggesting that the differing economic activities in these areas  
35 generate very different heavy metal pollutant loads (e.g. Hg dominated agricultural  
36 pollution vs. Pb dominated industrial pollution). In addition, all of the elements  
37 barring Hg have larger  $\Delta\alpha$ ,  $\Delta f(\alpha)$  and  $\tau''(1)$  values in the Daxing area compared to the  
38 Yicheng area. These larger values indicate that the higher concentrations of heavy  
39 metals present in soils within the Daxing area (compared to the Yicheng area) are  
40 more likely to be related to industrial activities than agriculture. The industrial Daxing  
41 area contains significant Pb and Cd soil contamination, whereas Hg is the main heavy  
42 metal present in soils within the Yicheng area, indicating that differing clean-up  
43 procedures and approaches to remediating these polluted areas are needed. The results  
44 also indicate that multifractal modeling and the associated generation of multifractal  
45 parameters can be a useful approach in the evaluation of heavy metal pollution in soils  
46 and the identification of major sources of heavy metal contamination.

47

48 **Keywords:** soil geochemistry; multifractal modelling, heavy metal pollution, Hefei.

49

## 50 **1. Introduction and overview of the study area**

51 Heavy metal pollution within soil poses a serious risk for human health and the  
52 environment, and thus soil pollution caused by anthropogenic activities (including  
53 industry and agriculture) has been the focus of a significant amount of research in  
54 recent years ([McGrath et al., 2004](#); [Wang et al., 2007](#); [Leyval et al., 1997](#); [Thomas](#)

55 [and Stefan, 2002; Luo et al., 2011](#)). Analyzing soil geochemistry and pollution using  
56 multifractal techniques has a lot of advantages, including the fact that these  
57 approaches can investigate many of the problems of nonlinear variability which  
58 commonly arise when dealing with pollutants and identify non-linear characteristics,  
59 yielding new information that can be used to understand the factors controlling the  
60 distribution of key elements within the objects or data being studied ([Salvadori, 1997;](#)  
61 [Gonçalves, 2000; Zuo et al., 2012](#)). This in turn means that using multifractal  
62 techniques to determine the multifractal characteristics of the distribution of heavy  
63 metals in soils can further our understanding of any heavy metal pollution that is  
64 associated with these differing activities.

65       Multifractal techniques include singularity mapping and multifractal  
66 interpolation that enable more detailed analysis of the spatial distribution of heavy  
67 metals, concentration-area modeling that can be used to define threshold values  
68 between background (i.e. geological) and anthropogenic anomalies ([Lima et al., 2003](#)),  
69 spectral density-area modeling that can be used to define thresholds to separate  
70 anomalies (i.e., anthropogenically derived heavy metal concentrations in this case)  
71 from background concentrations (i.e., geologically derived heavy metal  
72 concentrations; [Cheng, 2001](#)), and multifractal spectra that highlights non-linear  
73 characteristics and identifies anomalous behavior that reflects the characteristics of  
74 some multifractal sets ([Gonçalves, 2000; Albanese et al., 2007; Guillén et al., 2011](#)),  
75 such as identification of porous structures and the spatial variability in soil properties  
76 and so on ([Dathe et al., 2006; Caniego et al., 2005](#)). This means that multifractal  
77 techniques provide a lot of useful tools for the the analysis of heavy metals  
78 pollutantion within soils ([Lima et al., 2003; Albanese et al., 2007; Guillén et al., 2011;](#)  
79 [Salvadori et al., 1997](#)). These multifractal techniques are not only used in  
80 environmental science, but also be used in a number of differing fields, including  
81 geophysics ([Schertzer et al., 2011](#)), medicine ([Jennane et al., 2001](#)), computer science  
82 ([Wendt et al., 2009](#)), geology ([Deng et al., 2011; Zuo et al., 2012, 2014; Cheng, 1995;](#)  
83 [Nazarpour et al., 2014; Yuan et al., 2012, 2015](#)) and ecology ([Scheuring and Riedi,](#)  
84 [1994; Pascual et al., 1995](#)), among others.

85 Hefei is the capital of Anhui Province, China, and has an urban area that includes  
86 the towns of Daxing and Yicheng, which focus on industrial and agricultural activities,  
87 respectively. Here, we use multifractal techniques to determine the multifractal  
88 characteristics of the distribution of heavy metals in soils in these areas, using three  
89 multifractal parameters ( $\Delta\alpha$ ,  $\Delta f(\alpha)$  and  $\tau''(1)$ ) to analyze and compare the degree and  
90 characteristics of the multifractality of heavy metal contamination in soils associated  
91 with the anthropogenic activities in this region. The results will further enable and  
92 inform future planning for any necessary remediation of these soils in the Daxing and  
93 Yicheng areas.

## 94 **2. Study area and geochemical data**

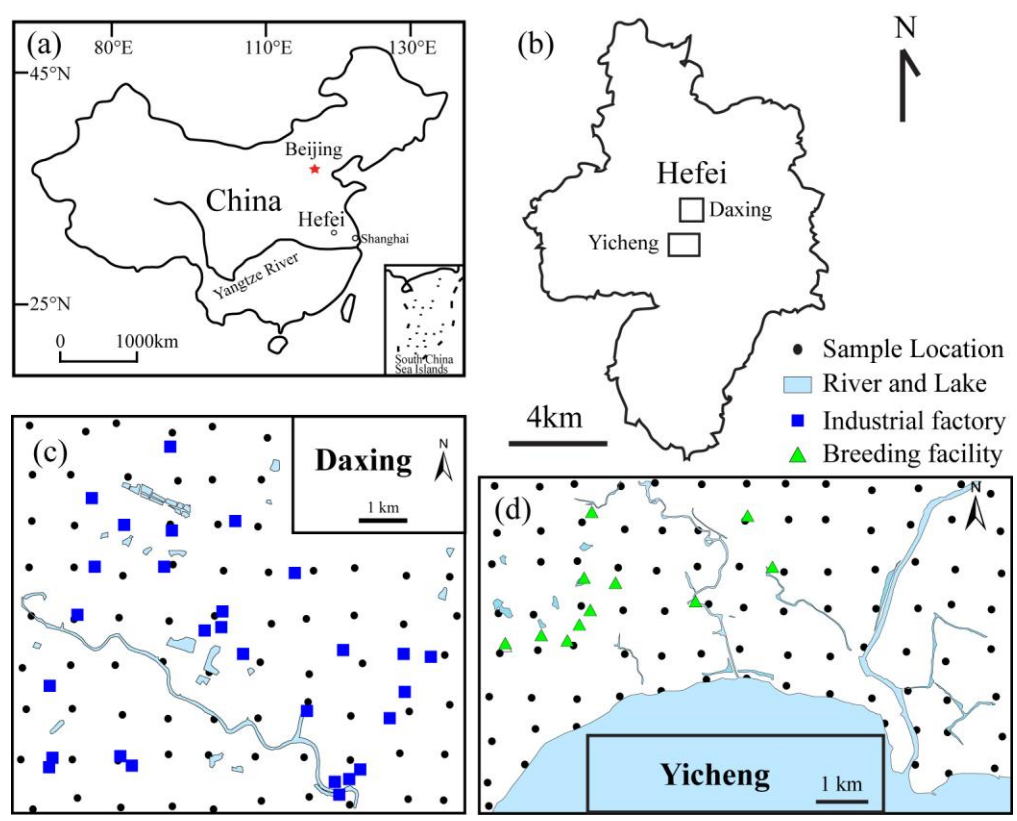
### 95 **2.1 Study area**

96 The city of Hefei is situated in central–eastern China (Fig. 1(a)), has  
97 approximately 7.7 million inhabitants and covers an area of around 11,408 km<sup>2</sup>. This  
98 paper focuses on the towns of Daxing and Yicheng (Fig. 1(b)), with the former  
99 representing one of the traditional industrial areas of Hefei and containing numerous  
100 factories that are involved in the steel industry, chemical industry, paper making, and  
101 the production of furniture and construction materials, among others. In contrast, the  
102 town of Yicheng focuses its economic activities on agricultural production, byproduct  
103 processing, livestock and poultry breeding, ornamentals, and other enterprises related  
104 to agricultural activity.

### 105 **2.2 Sampling and analysis**

106 The study areas are covered by Quaternary sedimentary soils and are free of both  
107 natural mineralization and mining-related contamination. A total of 169 surface (<20  
108 cm depth) soil samples were taken from the towns of Daxing and Yicheng on 1 × 1  
109 km grids, yielding 78 samples from Daxing and 91 samples from Yicheng (Fig.  
110 1(c–d)). Sampling errors were minimized by splitting each sample into 3–5  
111 sub-samples, each of which weighed more than 500 g. Each of these sub-samples was  
112 air-dried before being broken up using a wooden roller and then sieved to pass  
113 through a 0.85 mm mesh. The concentrations of 6 heavy metal elements (Cu, Pb, Zn,

114 Cd, As and Hg) were determined during this study, with Cd, Cu, Pb and Zn  
 115 concentrations determined by inductively coupled plasma–mass spectrometry  
 116 (ICP–MS) and Hg and As concentrations determined by hydride generation–atomic  
 117 fluorescence spectrometry (AFS). These techniques have detection limits of 1 ppm for  
 118 Cu, 2 ppm for Pb and Zn, 30 ppb for Cd, 0.5 ppm for As and 5 ppb for Hg. The  
 119 accuracy of these data was monitored by repeat determinations of standards and  
 120 replicate determinations of sub-sets of samples using instrumental neutron activation  
 121 analysis (INAA). Analytical precision was monitored using determinations of  
 122 variance of the results obtained from duplicate analyses.  
 123



124  
 125  
 126 **Fig.1.** Location of Hefei in central-eastern China (a); location of the study areas within Hefei (b);  
 127 the 1 x 1 km grids used for soil sampling in the towns of Daxing (c) and Yicheng (d)  
 128

129 **3. Multifractal spectrum analysis**

130 Multifractal formalisms can decompose self-similar measures into intertwined  
 131 fractal sets that are characterized by singularity strength and fractal dimensions

132 (Cheng, 1999). Using multifractal techniques allows non-linear characteristics within  
 133 datasets to be identified, enabling the extraction of information that can be used to  
 134 understand the factors controlling the distribution of key elements within the data.  
 135 Fractal spectra ( $f(\alpha)$ ) are formalisms that can be used to describe the multifractal  
 136 characteristics of a dataset and can be estimated using box-counting based moment,  
 137 gliding box, histogram and wavelet methods, among others (Cheng, 1999; Lopes and  
 138 Betrouni, 2009). The most widely used of these methods are the box-counting and  
 139 gliding box methods, both of which are based on the moment method.

140 The initial step of the box-counting method estimates mass exponent function  $\tau(q)$   
 141 values using a partition function as follows (Halsey et al., 1986):

$$142 \quad \tau(q) = \lim_{\varepsilon \rightarrow 0} \left( \frac{\log(\chi^q(\varepsilon))}{\log(\varepsilon)} \right) = \lim_{\varepsilon \rightarrow 0} \left( \frac{\log \left( \sum_{i=1}^{N(\varepsilon)} \mu_i^q(\varepsilon) \right)}{\log(\varepsilon)} \right) \quad (1)$$

143 where  $\mu_i(\varepsilon)$  denotes a measure with the  $i_{th}$  box of size  $\varepsilon$  and  $N(\varepsilon)$  indicates the total  
 144 number of boxes of size  $\varepsilon$  with  $\mu_i(\varepsilon)$  values different from 0.

145 The calculation of the mass exponent function  $\tau(q)$  for the gliding box method is  
 146 different from the box-counting method, with the gliding box method providing a  
 147 useful approach that can increase the number of samples that are available for  
 148 statistical estimation within a dataset (Tarquis et al., 2006; Xie et al., 2010;  
 149 Buczkowski et al., 1998). This means that the gliding box approach often provides  
 150 better results with lower uncertainties than the box-counting method (Cheng, 1999).  
 151 As such, we have used the gliding box approach during this study.

152 The calculation of the mass exponent function  $\tau(q)$  for the gliding box method  
 153 uses a partition function as follows (Cheng, 1999):

$$154 \quad \langle \tau(q) \rangle + D = \lim_{\varepsilon \rightarrow 0} \left( \frac{\log(\mu^q(\varepsilon))}{\log(\varepsilon)} \right) = \lim_{\varepsilon \rightarrow 0} \left( \frac{\log \left( \sum_{i=1}^{N^*(\varepsilon)} \mu_i^q(\varepsilon) \right)}{\log(\varepsilon)} \right) \quad (2)$$

155 where  $\mu_i(\varepsilon)$  denotes a measure with the  $i_{th}$  cell of a gliding box of size  $\varepsilon$ ,  $\langle \rangle$  indicates  
 156 the statistical moment, and  $N^*(\varepsilon)$  indicates the total number of gliding boxes of size  $\varepsilon$   
 157 with  $\mu_i(\varepsilon)$  values different from 0.

158 The values of  $\tau(q)$  derived using this equation can be then used to determine  $\alpha$   
 159 and  $f(\alpha)$  values using a Legendre transformation, as expressed below:

$$160 \quad \alpha(q) = \frac{d\tau(q)}{dq} \quad (3)$$

$$161 \quad f(q) = q\alpha(q) - \tau(q) = q \frac{d\tau(q)}{dq} - \tau(q) \quad (4)$$

162 where  $\Delta\alpha$  and  $\Delta f$  are essential parameters required to analyze the multifractal  
 163 characteristics of the dataset in question. The widths of the left and right branches  
 164 within the multifractal spectra are then defined using the following equations:

$$165 \quad \Delta\alpha_L = \alpha_0 - \alpha_{\text{min}} \quad (5)$$

$$166 \quad \Delta\alpha_R = \alpha_{\text{max}} - \alpha_0 \quad (6)$$

$$167 \quad \Delta\alpha = \alpha_{\text{max}} - \alpha_{\text{min}} \quad (7)$$

168 and the height difference  $\Delta f(\alpha)$  between the two ends of the multifractal spectrum is  
 169 then extracted using:

$$170 \quad \Delta f(\alpha) = f(\alpha_{\text{max}}) - f(\alpha_{\text{min}}) \quad (8)$$

171 Higher  $\Delta\alpha$  and  $\Delta f(\alpha)$  values are generally indicative of datasets with more  
 172 heterogeneous patterns and higher levels of multifractality (Cheng, 1999; Kravchenko  
 173 et al., 1999). In addition, multifractality associated with ordinary spatial analysis  
 174 parameters, as represented by the  $\tau''(1)$  parameter, can also be used as a measure to  
 175 quantitatively characterize the multifractality of a dataset (Cheng, 2006) using the  
 176 following equation:

$$177 \quad \tau''(1) = \tau(2) - 2\tau(1) + \tau(0) \quad (9)$$

178 If  $\mu$  is a multifractal and  $-D < \tau''(1) < 0$ , where  $D$  is the box-counting dimension,  
 179 then smaller values of  $\tau''(1)$  are indicative of higher degrees of multifractality,  
 180 whereas otherwise  $\tau''(1) = 0$  for a single fractal.

181 Here, we use the three multifractal parameters described above ( $\Delta\alpha$ ,  $\Delta f(\alpha)$  and  
 182  $\tau''(1)$ ) to better identify heterogeneous patterns and the degrees of multifractality  
 183 within the soil geochemical data for the study area as well as enabling the comparison

184 of the distribution of differing elements in the soils in this region.

#### 185 **4. Geochemical analysis results**

186 A statistical summary of the soil geochemical data for the study area are given in  
187 [Table 1](#). Samples from Daxing have higher Cu, Pb, Zn, Cd and As maximum,  
188 standard deviation, skewness, and kurtosis values than soil samples from the Yicheng  
189 area. In addition, the soil samples from Daxing have much higher coefficient of  
190 variation (CV) values for Cu, Pb, Zn, Cd and As than the samples from the Yicheng  
191 area, indicating that soils in the Daxing area contain much higher and more variable  
192 concentrations of these elements. This also suggests that samples from the Daxing  
193 area containing elevated concentrations of heavy metals were probably contaminated  
194 by anthropogenic activity.

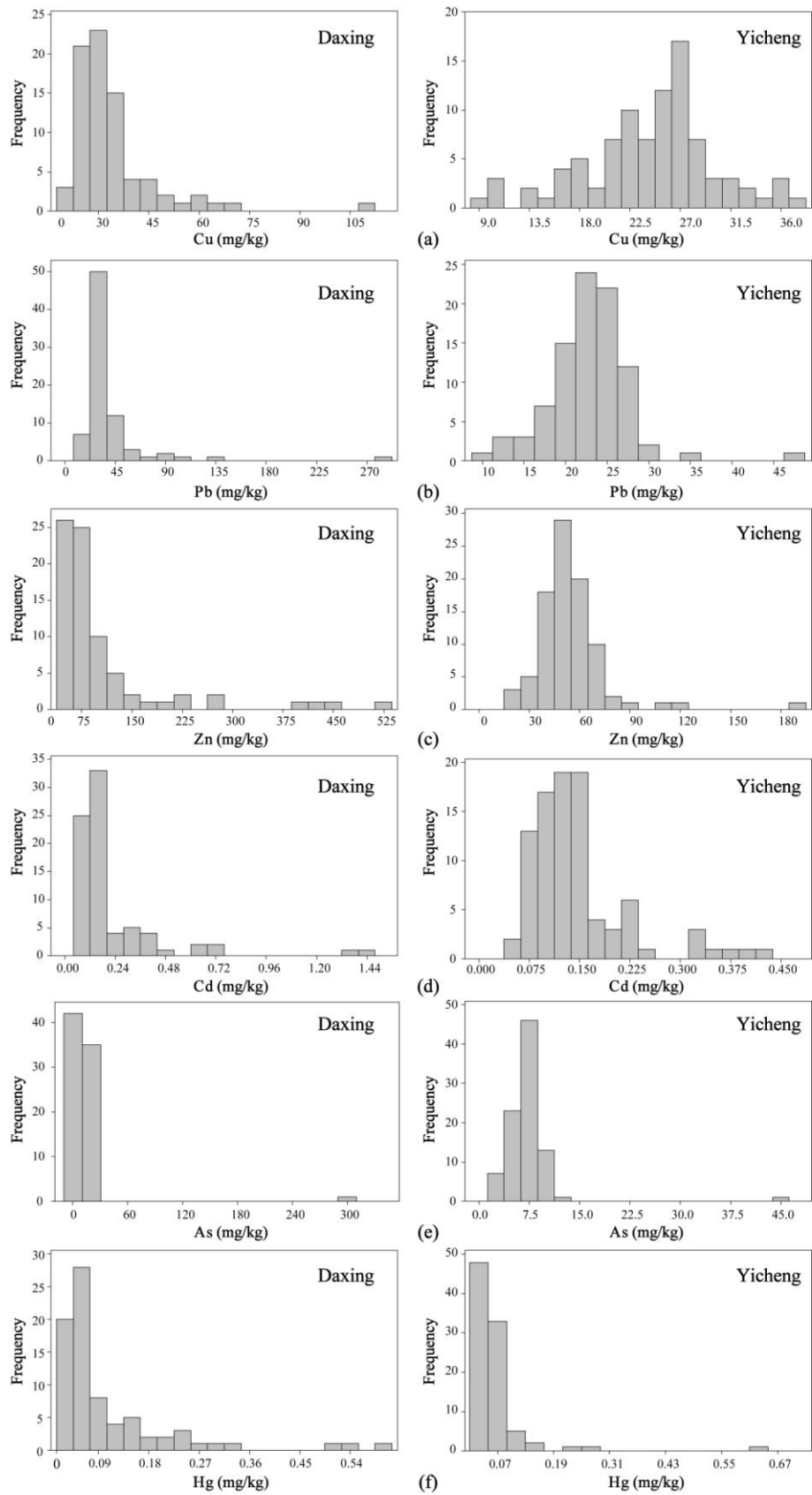
195 All of the elements (barring Pb and Cu in the Yicheng area) in both the Yicheng  
196 and Daxing areas yield histograms that are positively skewed and contain some  
197 outliers (Fig. 2), indicating that these data have non-normal and potentially fractal- or  
198 multifractal-type distributions. This means that multifractal techniques are highly  
199 suited for the characterization of the geochemistry of the contaminated soils in these  
200 areas.

201

202 Table 1. Summary statistics of soil heavy metal concentrations within samples from the Daxing  
203 and Yicheng areas.

Town	Element	Min	Max	Mean	Standard deviation	Skewness	Kurtosis	CV*
		(mg/kg)	(mg/kg)	(mg/kg)	-	-	-	(%)
Daxing	Cu	19.00	111.50	33.87	13.26	3.20	14.93	39.16
	Pb	18.90	291.30	39.57	35.03	5.37	35.41	88.51
	Zn	40.90	526.10	105.8	94.40	2.91	8.59	89.19
	Cd	0.045	1.48	0.23	0.24	3.45	13.81	108.23
	As	4.93	308.20	13.97	33.89	8.72	76.64	242.56
	Hg	0.03	0.60	0.11	0.11	2.68	7.78	107.29
Yicheng	Cu	9.60	37.80	24.34	5.77	-0.38	0.41	23.71
	Pb	10.40	46.30	22.77	4.91	0.87	5.51	21.56
	Zn	20.80	194.80	54.70	21.43	3.45	20.27	39.17
	Cd	0.054	0.43	0.15	0.08	1.84	3.49	51.85
	As	2.30	44.20	7.29	4.39	6.68	56.55	60.24
	Hg	0.02	0.62	0.06	0.07	5.75	41.26	113.09





205

206

207

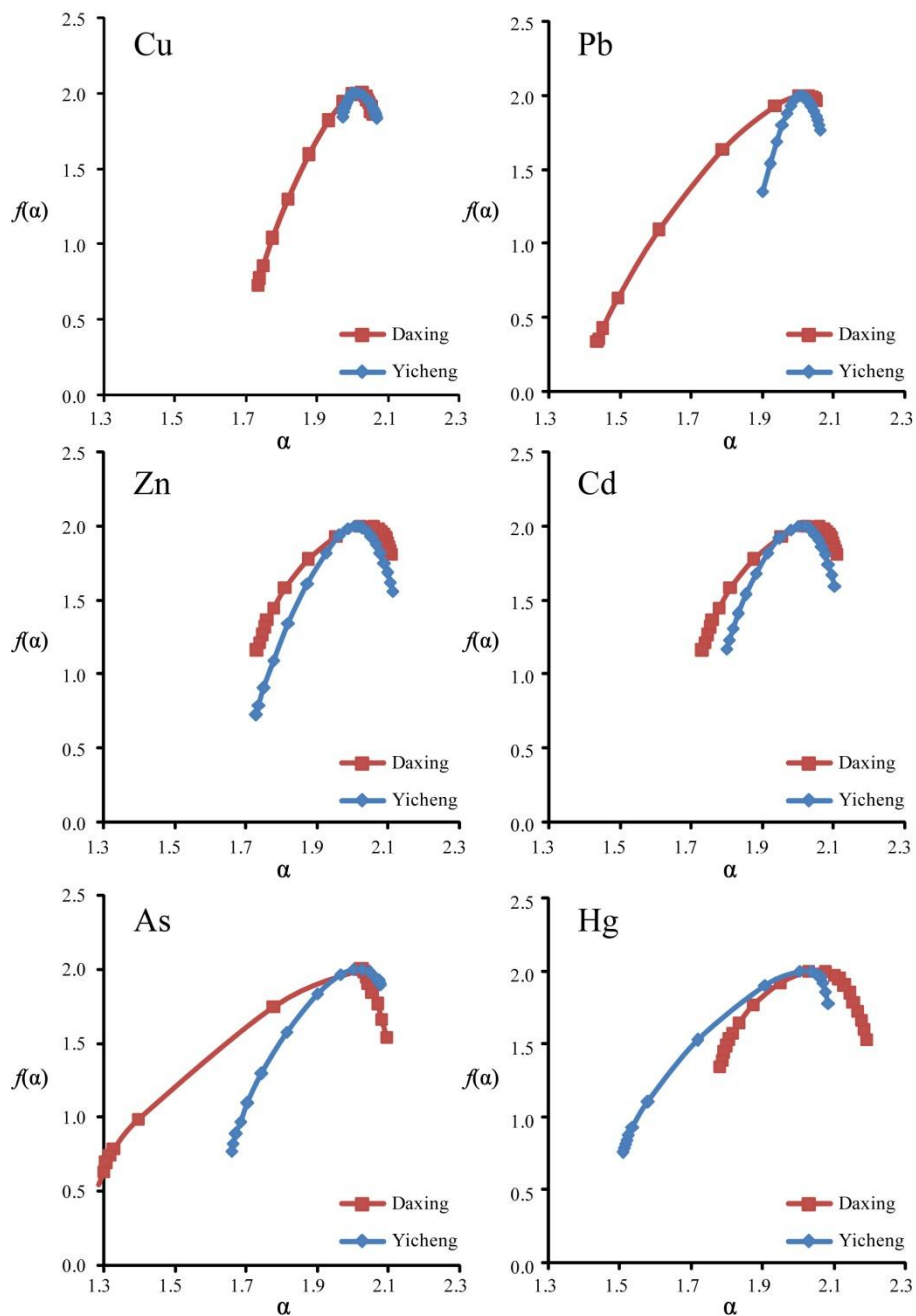
**Fig. 2.** Histograms showing the distribution of Cu (a), Pb (b), Zn (c), Cd (d), As (e) and Hg (f) concentrations within soils from the towns of Daxing and Yicheng.

208

## 209 5. Calculation processes of multifractal spectrum and discussion

210 Here, we use the gliding box method to calculate multifractal spectra for the  
211 geochemical data from the study area. This calculation used a range of  $q$  values from  
212  $-10$  to  $10$  with an interval of  $1$ , yielding the multifractal spectra (in the form of an  $\alpha$ - $f$   
213 ( $\alpha$ ) diagram) shown in Fig. 3.

214



215

216 **Fig. 3.** Multifractal spectra ( $f(\alpha)$  vs  $\alpha$ ) showing the multifractal characteristics of all of the soil

217 geochemical data (barring Cu) from the Yichen area.

218

219 Multifractal spectra combine the singularity exponent  $\alpha$  and the corresponding  
220 fractal dimension  $f(\alpha)$  to generate a multifractal spectrum with an inverse bell shape  
221 (Fig. 3). All of these multifractal spectra are also asymmetric ( $\Delta\alpha_L$  is significantly  
222 different from  $\Delta\alpha_R$ , equations 5-6) (barring the Cu data for soils from the Yicheng  
223 area), indicating that the soils containing low and high concentrations of these  
224 elements are not evenly distributed within the study area (as is expected for areas  
225 containing point source pollutants like factories or animal breeding facilities).

226 The multifractal analytical results shown in Table 2 indicate that all of the  
227 elements (barring Cu in the Yicheng area) are characterized by a wide range of  $\alpha$   
228 values (i.e. have high  $\Delta\alpha$  values), have  $\tau''(1)$  values less than  $-0.01$  (barring Cu and  
229 Pb in the Yicheng area) and have  $\Delta f(\alpha)$  values larger than  $0.5$  (barring Cu in the  
230 Yicheng area), all of which indicate that these elements have highly multifractality  
231 within the soils in these two areas. All of the elements analyzed during this study  
232 (barring Hg) have higher  $\Delta f(\alpha)$  and  $\alpha$  values (except Zn) and lower  $\tau''(1)$  values in  
233 soils from the Daxing area, with Hg having higher  $\Delta f(\alpha)$  and  $\alpha$  and lower  $\tau''(1)$  values  
234 in soils from the Yicheng area (Table 2). This suggests that the industrial activities in  
235 the Daxing area generate multi-element heavy metal soil contamination, whereas the  
236 significant heavy metal pollution associated with the agricultural activity in the  
237 Yicheng area would be Hg contamination. The  $\Delta f(\alpha)$  and  $\alpha$  values of Hg in Yicheng  
238 area are larger than all of the other elements in this area as well as some of the  
239 elements in the Daxing area, indicating both the prevalence and significant degree of  
240 agricultural Hg contamination in the Yicheng area. This is important, primarily as Hg  
241 pollution can seriously impact human health because this element is preferentially  
242 concentrated upward in the food chain (e.g. (Jiang et al., 2006)), meaning that this  
243 contamination needs to be evaluated further and remediated to avoid any deleterious  
244 effects.

245

246 **Table 2.** Multifractal parameters of the elements within the soil samples analyzed during this  
247 study.

Town	Element	$\alpha_{\min}$	$\alpha_{\max}$	$\Delta\alpha_L$	$\Delta\alpha_R$	$\Delta\alpha$	$\Delta f(\alpha)$	$\tau''(1)$
Daxing	Cu	1.733	2.057	0.280	0.044	0.324	1.270	-0.015
	Pb	1.439	2.050	0.567	0.044	0.611	1.659	-0.068
	Zn	1.733	2.109	0.288	0.088	0.376	0.841	-0.066
	Cd	1.482	2.285	0.499	0.304	0.803	1.358	-0.066
	As	1.285	2.094	0.739	0.070	0.809	1.490	-0.243
	Hg	1.780	2.191	0.248	0.163	0.411	0.656	-0.079
Yicheng	Cu	1.971	2.067	0.036	0.060	0.096	0.168	-0.007
	Pb	1.900	2.062	0.104	0.058	0.162	0.646	-0.005
	Zn	1.729	2.112	0.275	0.108	0.383	1.275	-0.016
	Cd	1.800	2.103	0.201	0.102	0.303	0.829	-0.023
	As	1.659	2.076	0.343	0.075	0.418	1.224	-0.036
	Hg	1.507	2.084	0.497	0.080	0.577	1.243	-0.096

248

249 Different elements were sorted by  $\Delta\alpha$ ,  $\Delta f(\alpha)$  and  $\tau''(1)$  parameters in order to  
250 compare variations in multifractality, in addition to sorting by basic statistics such as  
251 standard deviation and coefficient of variation values (Table 3). The data shown in  
252 Table 3 indicates that the Zn data within the Daxing area has largest standard  
253 deviation value but only a moderate coefficient of variation, but the  $\Delta\alpha$  and  $\Delta f(\alpha)$   
254 values for these Zn data are indicative of only weak multifractality compared to the  
255 other heavy metals in the soils of the Daxing area. In comparison, the Hg data for  
256 soils in the Yicheng area yielded the lowest standard deviation value but the largest  
257  $\Delta\alpha$  and  $\tau''(1)$  values, indicating these Hg data have strong multifractality. These  
258 differences indicate that the multifractal parameters  $\Delta\alpha$ ,  $\Delta f(\alpha)$  and  $\tau''(1)$  reveal new  
259 information about the nonlinear variability and the characteristics of these  
260 geochemical data compared to the analyses afforded by classic basic statistics. In  
261 addition, the data given in Table 3 indicates that these elements have different orders  
262 depending on whether they are sorted by  $\Delta\alpha$ ,  $\Delta f(\alpha)$  or by  $\tau''(1)$  values, all of which  
263 reflects differing aspects of the multifractality of these data. Here we first averaged  
264 the ordering of these elements by  $\Delta\alpha$ ,  $\Delta f(\alpha)$  and  $\tau''(1)$  before sorting again to compare  
265 the overall multifractality of these data.

266

267 **Table 3.** Elements sorted by multifractal parameters and coefficient of variation values.

Town	Element	Order
------	---------	-------

		Basic statistics		Multifractal parameters			Overall*
		Standard deviation	Coefficient of variation	$\Delta\alpha$	$\Delta f(\alpha)$	$\tau''(1)$	
<b>Daxing</b>	Cu	4	6	6	4	6	6
	Pb	2	5	3	1	1	1
	Zn	1	4	5	5	2	4
	Cd	5	2	2	3	3	2
	As	3	1	1	2	5	3
	Hg	6	3	4	6	4	5
<b>Yicheng</b>	Cu	2	5	6	6	5	6
	Pb	3	6	5	5	6	5
	Zn	1	4	3	1	4	3
	Cd	5	3	4	4	3	4
	As	4	2	2	3	2	2
	Hg	6	1	1	2	1	1

268 Overall: the overall order of  $\Delta\alpha$ ,  $\Delta f(\alpha)$  and  $\tau''(1)$

269

270 The overall amount of multifractality within the soil geochemical data for the  
 271 Daxing area decreases as follows: Pb>Cd>As>Zn>Hg>Cu, whereas the overall  
 272 amount of multifractality within the soil geochemical data for the Yicheng area  
 273 decreases as follows: Hg>Zn>As>Cd>Pb>Cu. The overall orders indicates that the Pb  
 274 and Hg soil data have the highest degree of multifractality in the Daxing and Yicheng  
 275 areas, respectively, whereas Cu has the weakest multifractality irrespective of the  
 276 area.

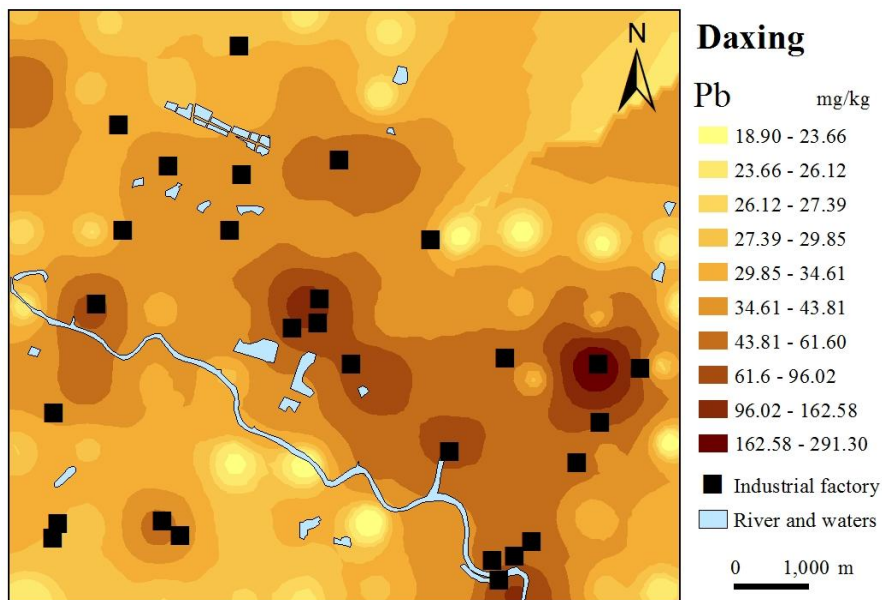
277 We further analyzed the spatial distribution of contamination within soils from  
 278 the Daxing and Yicheng areas and evaluated whether there is any significant  
 279 correlation between multifractality and anthropogenic activity. Filled contour maps  
 280 showing the distribution of Pb in the Daxing area and Hg and Cu in the Yicheng area  
 281 were calculated using inverse distance weighted interpolation (Fig. 4–6). These maps  
 282 indicate that areas with elevated levels of Pb contamination within the Daxing area  
 283 are directly correlated to the location of industrial factories, whereas the Hg  
 284 contamination in the Yicheng area is spatially correlated with the location of  
 285 agricultural breeding facilities. The Hg contamination in the Yicheng area is of  
 286 significance, especially as this form of contamination can cause serious health issues

287 (e.g. Minamata disease). As such, the soils in this area may well require remediation,  
288 especially as Hg can be concentrated up the food chain and the Yicheng area is  
289 heavily agricultural, indicating that this activity may both be concentrating Hg as well  
290 as contaminating soils in this area.

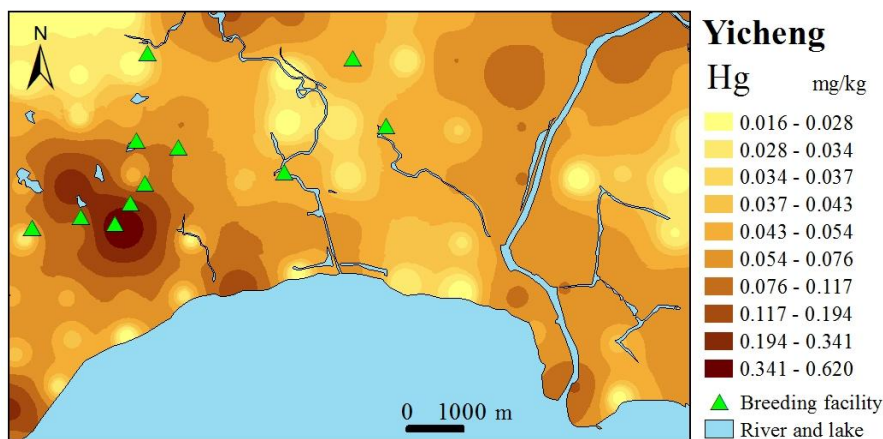
291 This distribution of soils with elevated concentrations of Hg also contrasts with  
292 the symmetrical distribution and weakest multifractality for Cu within the Yicheng  
293 area (Fig. 3, 5-6). We used a plot showing the rank of concentration contour vs  
294 number of agricultural facilities within the same rank of concentration contour to  
295 demonstrate the spatial correlation between the location of agricultural facilities and  
296 heavy metal concentrations in soils (Fig. 7). This diagram shows an significant  
297 correlation between agricultural facilities and high concentrations of Hg, whereas  
298 there is an anti-correlation when comparing agricultural breeding facilities and areas  
299 of high Cu concentrations. This indicates that very little Cu has been  
300 anthropogenically added (or removed) from the soils in the Yicheng area, suggesting  
301 that these soils maybe contain only natural background concentrations of Cu and that  
302 the agricultural activity in this area does not produce significant Cu contamination.

303 All of the above suggests that the multifractal parameters for the heavy metal  
304 concentrations within soil geochemical data can efficiently reflect the multifractality  
305 associated with by industrial and agricultural activities in the Daxing and Yicheng  
306 areas, respectively. These results also indicate that multifractal modeling and the  
307 associated generation of multifractal parameters are a useful approach in the  
308 evaluation of heavy metal pollution in soils and the identification of major element of  
309 heavy metal contamination. In addition, the differing orders of the geochemical data  
310 for soils within the Daxing area and Yicheng area are indicative of a significant  
311 difference in the geochemical characteristics (and heavy metal pollution) in the soils  
312 within these two areas. This indicates that differing clean-up procedures and  
313 approaches to remediating these polluted areas are needed, rather than a single  
314 cover-all approach to the remediation of heavy metal pollution. A significant amount  
315 of different remediation approaches can be used to resolve the issues of heavy metal  
316 soil contamination (e.g., Bech et al., 2014; Koptsik, 2014), with the results presented

317 in this study suggesting that physical and chemical approaches (soil removal, soil  
 318 vitrification, soil consolidation, electroremediation, soil washing) are more  
 319 appropriate for the remediation of heavy metal contaminated soil in the Daxing area,  
 320 especially in areas with significant heavy metal pollution. In comparison, the differing  
 321 (i.e. Hg-dominated) type of soil contamination in the Yicheng area could be more  
 322 efficiently treated using microremediation and phytoremediation, primarily as the  
 323 agriculture in this area requires a rapid reduction in the mobility and biological  
 324 availability of heavy metals in the soils in this area (Mulligan et al., 2001; Wang et al.,  
 325 2006).  
 326

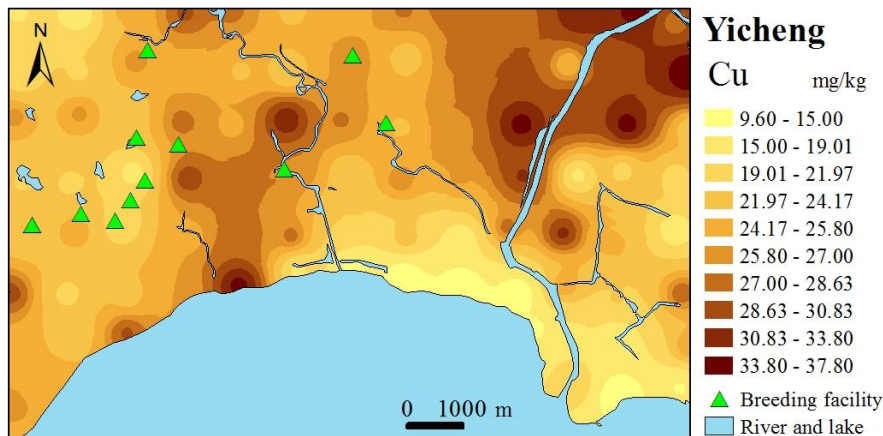


327  
 328 **Fig. 4.** Filled contour map generated by inverse distance weighted interpolation showing the  
 329 spatial distribution of soil Pb concentrations in the Daxing area.  
 330

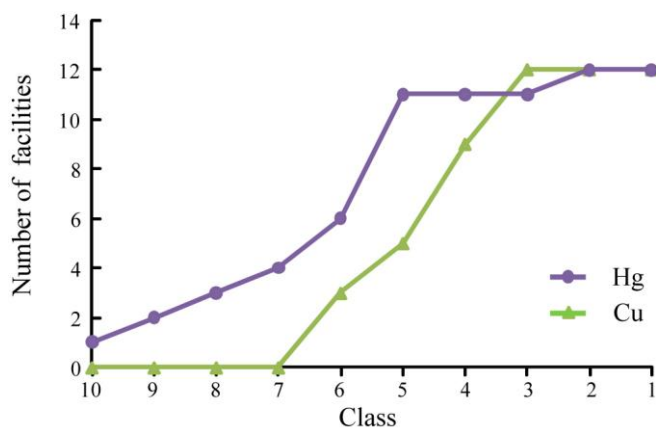


331

332 **Fig. 5.** Filled contour map generated by inverse distance weighted interpolation showing the  
 333 spatial distribution of soil Hg concentrations in the Yicheng area.



334 **Fig. 6.** Filled contour map generated by inverse distance weighted interpolation showing the  
 335 spatial distribution of soil Cu concentrations and the location of breeding facilities in the Yicheng  
 336 area  
 337



339 **Fig. 7.** Plot of number of agricultural facilities in Yicheng area within the same rank of Hg  
 340 and Cu concentration contour showing a positive spatial correlation between location of  
 341 agricultural facilities and Hg concentrations but an anti-correlation between the location of  
 342 agricultural facilities and Cu concentrations.  
 343  
 344

## 345 5. Conclusions

346 This study focuses on the geochemistry of heavy metal contaminated soils from  
 347 the Daxing and Yicheng areas, both of which are located close to the city of Hefei, in  
 348 Anhui Province, China. Multifractal modelling and the resulting multifractal  
 349 parameters indicate that the soils from the Daxing area have stronger multifractality  
 350 for Cu, Pb, Zn, Cd and As than soils from the Yicheng area, although the latter have  
 351 relatively strong multifractality for Hg. The ordering of values for the multifractal



352 parameters  $\Delta\alpha$ ,  $\Delta f(\alpha)$  and  $\tau''(1)$  indicate the degree of multifractality for the  
353 geochemical data for soils within the Daxing area descends as follows:  
354 Pb>Cd>As>Zn>Hg>Cu, whereas the overall order in soils within the Yicheng area  
355 descends as follows: Hg>Zn>As>Cd>Pb>Cu. In addition, Cu concentrations in soils  
356 in the Yicheng area may still have their original (i.e. natural) distribution and may not  
357 have been influenced by human activities. These data indicate that the industrial  
358 activity concentrated in the Daxing area generates multi-element heavy metal soil  
359 contamination whereas the agricultural activity concentrated in the Yicheng area  
360 generates Hg-dominated heavy metal soil contamination. The latter is important, as  
361 Hg contamination can cause serious health issues (e.g. Minamata disease) and the  
362 soils in this area may well require remediation, especially as Hg can be concentrated  
363 up the food chain and the Yicheng area is heavily agricultural, indicating that this  
364 activity may both be concentrating Hg as well as contaminating soils in this area.

365 The initial results presented here indicate that multifractal modeling and the  
366 associated generation of multifractal parameters can efficiently reflect the  
367 multifractality caused by industrial and agricultural activities in the Daxing and  
368 Yicheng areas, respectively. This in turn indicates that multifractal modeling can be a  
369 useful approach in the evaluation of heavy metal pollution in soils and the  
370 identification of major sources of heavy metal contamination.

### 371 **Acknowledgements**

372 This research was financially supported by funds from the Fundamental Research  
373 Funds for the Central Universities, the China Academy of Science "Light of West  
374 China" Program, and the Programme for New Century Excellent Talents in University  
375 (Grant No. NCET-10-0324).

### 376 **References**

- 377 Albanese, S., De Vivo, B., Lima, A., and Cicchella, D.: Geochemical background and  
378 baseline values of toxic elements in stream sediments of Campania region (Italy),  
379 Journal of Geochemical Exploration, 93, 21-34, 2007.
- 380 Bech, J., Korobova, E., Abreu, M., Bini, C., Chon, H. T., and Pérez-Sirvent, C.: Soil

381 pollution and reclamation, *Journal of Geochemical Exploration*, 147, 77-79, 2014.

382 Buczkowski, S., Hildgen, P., and Cartilier, L.: Measurements of fractal dimension by  
383 box-counting: a critical analysis of data scatter, *Physica A Statistical Mechanics &*  
384 *Its Applications*, 252, 23–34, 1998.

385 Caniego, F. J., Espejo, R., Martín, M. A., and José, F. S.: Multifractal scaling of soil  
386 spatial variability, *Ecological Modelling*, 182, 291-303, 2005.

387 Cheng, Q.: The perimeter-area fractal model and its application to geology,  
388 *Mathematical Geology*, 27, 69-82, 1995.

389 Cheng, Q.: The gliding box method for multifractal modeling, *Computer &*  
390 *Geosciences*, 25, 1073-1079, 1999.

391 Cheng, Q.: Selection of Multifractal Scaling Breaks and Separation of Geochemical  
392 and Geophysical Anomaly, *Journal of China University of Geosciences*, 1, 54-59,  
393 2001.

394 Cheng, Q.: Multifractal modelling and spectrum analysis: Methods and applications to  
395 gamma ray spectrometer data from southwestern Nova Scotia, Canada, *Science in*  
396 *China Series D: Earth Sciences*, 49, 283-294, 2006.

397 Dathe, A., Tarquis, A. M., and Perrier, E.: Multifractal analysis of the pore- and  
398 solid-phases in binary two-dimensional images of natural porous structures,  
399 *Geoderma*, 134, 318–326, 2006.

400 Deng, J., Wang, Q., Wan, L., Liu, H., Yang, L., and Zhang, J.: A multifractal analysis  
401 of mineralization characteristics of the Dayingezhuang disseminated-veinlet gold  
402 deposit in the Jiaodong gold province of China, *Ore Geology Reviews*, 40, 54–64,  
403 2011.

404 Gonçalves, M. A.: Characterization of Geochemical Distributions Using Multifractal  
405 Models, *Mathematical Geology*, 33, 41-61, 2000.

406 Guillén, M. T., Delgado, J., Albanese, S., Nieto, J. M., Lima, A., and De Vivo, B.:  
407 Environmental geochemical mapping of Huelva municipality soils (SW Spain) as  
408 a tool to determine background and baseline values, *Journal of Geochemical*  
409 *Exploration*, 109, 59-69, 2011.

410 Halsey, T.C., Jensen, M.H., Kadano, L.P., Procaccia, I., and Shraiman, B.I.: Fractal

411 measures and their singularities: the characterization of strange sets. *Physical*  
412 *Review*, A, 33 (2), 1141-1151, 1986.

413 Jennane, R., Ohley, W. J., Majumdar, S., and Lemineur, G.: Fractal analysis of bone  
414 X-ray tomographic microscopy projections, *IEEE Transactions on Medical*  
415 *Imaging*, 20, 443-449, 2001.

416 Jiang, G. B., Shi, J. B., and Feng, X. B.: Mercury Pollution in China, *Environmental*  
417 *Science & Technology*, 40, 3672-3678, 2006.

418 Koptsik, G. N.: Modern approaches to remediation of heavy metal polluted soils: A  
419 review, *Eurasian Soil Science*, 47, 707-722, 2014.

420 Kravchenko, A., Boast, C., and Bullock, D.: Multifractal analysis of soil spatial  
421 variability, *Agronomy Journal*, 91, 1033-1041, 1999.

422 Leyval, C., Turnau, K., and Haselwandter, K.: Effect of heavy metal pollution on  
423 mycorrhizal colonization and function: physiological, ecological and applied  
424 aspects, *Mycorrhiza*, 7, 139-153, 1997.

425 Lima, A., De Vivo, B., Cicchella, D., Cortini, M., and Albanese, S.: Multifractal IDW  
426 interpolation and fractal filtering method in environmental studies: an application  
427 on regional stream sediments of (Italy), Campania region, *Applied Geochemistry*,  
428 18, 1853-1865, 2003.

429 Lopes, R., and Betrouni, N.: Fractal and multifractal analysis: A review, *Medical*  
430 *Image Analysis*, 13, 634-649, 2009.

431 Luo, C., Liu, C., Yan, W., Xiang, L., Li, F., Gan, Z., and Li, X.: Heavy metal  
432 contamination in soils and vegetables near an e-waste processing site, South  
433 China, *Journal of Hazardous Materials*, 186, 481-490, 2011.

434 Mulligan, C., Yong, R., and Gibbs, B. F.: Remediation technologies for  
435 metal-contaminated soils and groundwater: an evaluation. *Engineering Geology*,  
436 60, 193-207, 2001,

437 McGrath, D., Zhang, C., and Carton, O. T.: Geostatistical analyses and hazard  
438 assessment on soil lead in Silvermines area, Ireland, *Environmental Pollution*,  
439 127, 239-248, 2004.

440 Nazarpour, A., Omran, N. R., Paydar, G. R., Sadeghi, B., Matroud, F., and Nejad, A.

441 M.: Application of classical statistics, logratio transformation and multifractal  
442 approaches to delineate geochemical anomalies in the Zarshuran gold district,  
443 NW Iran, *Chemie der Erde - Geochemistry*, 75, 117-132, 2014.

444 Pascual, M., Ascioti, F., and Caswell, H.: Intermittency in the plankton: a multifractal  
445 analysis of zooplankton biomass variability, *Journal of Plankton Research*, 17,  
446 167-168, 1995.

447 Salvadori, G., Ratti, S. P., and Belli, G.: Fractal and multifractal approach to  
448 environmental pollution, *Environmental Science & Pollution Research*, 4, 91-98,  
449 1997.

450 Schertzer, D., Lovejoy, S., Schmitt, F., Chigirinskaya, Y., and Marsan, D.: Multifractal  
451 Cascade Dynamics and Turbulent Intermittency, *Fractals-complex Geometry  
452 Patterns & Scaling in Nature & Society*, 5, 427-471, 2011.

453 Scheuring, I., and Riedi, R.: Application of multifractals to the analysis of vegetation  
454 pattern, *Journal of Vegetation Science*, 5, 489-489, 1994.

455 Tarquis, A. M., McInnes, K. J., Key, J. R., Saa, A., Garc á, M. R., and D áz, M. C.:  
456 Multiscaling analysis in a structured clay soil using 2D images, *Journal of  
457 Hydrology*, 322, 236-246, 2006.

458 Thomas, K., and Stefan, S.: Estimate of heavy metal contamination in soils after a  
459 mining accident using reflectance spectroscopy, *Environmental Science &  
460 Technology*, 36, 2742-2747, 2002.

461 Wang, Y., and Greger, M.: Use of iodide to enhance the phytoextraction of  
462 mercury-contaminated soil. *Science of the Total Environment*, 368, 30-39, 2006.

463 Wang, Y. P., Shi, J. Y., Wang, H., Lin, Q., Chen, X. C., and Chen, Y. X.: The influence  
464 of soil heavy metals pollution on soil microbial biomass, enzyme activity, and  
465 community composition near a copper smelter. *Ecotox Environ Safe,  
466 Ecotoxicology & Environmental Safety*, 67, 75-81, 2007.

467 Wendt, H., Roux, S. G., Jaffard, S., and Abry, P.: Wavelet leaders and bootstrap for  
468 multifractal analysis of images, *Signal Processing*, 89, 1100–1114, 2009.

469 Xie, S., Cheng, Q., Xing, X., Bao, Z., and Chen, Z.: Geochemical multifractal  
470 distribution patterns in sediments from ordered streams, *Geoderma*, 160, 36-46,

471 2010.

472 Yuan, F., Li, X., Jowitt, S. M., Zhang, M., Jia, C., Bai, X., and Zhou, T.: Anomaly  
473 identification in soil geochemistry using multifractal interpolation: A case study  
474 using the distribution of Cu and Au in soils from the Tongling mining district,  
475 Yangtze metallogenic belt, Anhui province, China, *Journal of Geochemical*  
476 *Exploration*, 116-117, 28-39, 2012.

477 Yuan, F., Li, X., Zhou, T., Deng, Y., Zhang, D., Xu, C., Zhang, R., Jia, C., and Jowitt,  
478 S. M.: Multifractal modelling-based mapping and identification of geochemical  
479 anomalies associated with Cu and Au mineralisation in the NW Junggar area of  
480 northern Xinjiang Province, China, *Journal of Geochemical Exploration*, 154,  
481 252-264, 2015.

482 Zuo, R., Carranza, E. J. M., and Cheng, Q.: Fractal/multifractal modelling of  
483 geochemical exploration data, *Journal of Geochemical Exploration*, 122, 1-3,  
484 2012.

485 Zuo, R.: Identification of geochemical anomalies associated with mineralization in the  
486 Fanshan district, Fujian, China, *Journal of Geochemical Exploration*, 139,  
487 170–176, 2014.